Journal of Hazardous Materials 389 (2020) 121853

Contents lists available at ScienceDirect

Journal of Hazardous Materials

journal homepage: www.elsevier.com/locate/jhazmat

Identifying bioaccessible suspect toxicants in sediment using adverse outcome pathway directed analysis

Fei Cheng[a,b,d], Huizhen Li[b], Huimin Ma[a], Fengchang Wu[c], Zhiyou Fu[c], Jing You[b,*]

[a] State Key Laboratory of Organic Geochemistry, Guangzhou Institute of Geochemistry, Chinese Academy of Sciences, Guangzhou, 510640, China
[b] Guangdong Key Laboratory of Environmental Pollution and Health, School of Environment, Jinan University, Guangzhou, 511443, China
[c] State Key Laboratory of Environment Criteria and Risk Assessment, Chinese Research Academy of Environmental Sciences, Beijing, 100012, China
[d] University of Chinese Academy of Sciences, Beijing, 100049, China

GRAPHICAL ABSTRACT

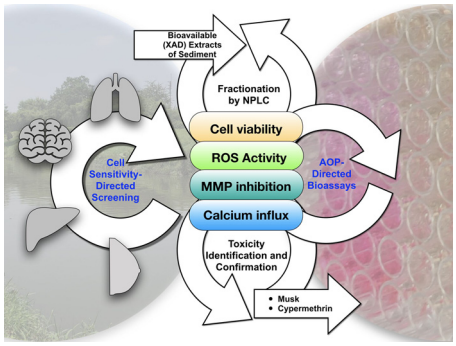

ARTICLE INFO

Editor: R. Debora

Keywords:
Effect-directed analysis
Bioaccessibility
Neurotoxicity
Adverse outcome pathway
Sediment

ABSTRACT

Chemical mixtures are a common occurrence in contaminated sediment and determining causal relationship between sediment contamination and adverse outcomes is challenging. The bioavailability and choice of bioassay endpoints played important roles in elucidating causality. As such, bioaccessibility-based XAD extraction and adverse outcome pathway (AOP) guided bioassays were incorporated into an effect-directed analysis to more effectively determine sediment causality. XAD extracts of sediments from urban waterways in Guangzhou, China were examined using cell viability bioassays with four human tumor cells from lung, liver, breast, and bone marrow. Pronounced effects to SH-SY5Y cells were noted, thus neurotoxicity was subsequently focused in the AOP-guided bioassays. Intracellular calcium influx, mitochondrial membrane potential inhibition, reactive oxygen species generation, and cell viability were utilized as evidence for neurotoxicity AOP-guided analysis. Suspect toxicants were identified in active fractions using GC–MS. Toxicity confirmation was performed by evaluating toxicity contributions of the candidates to the pathway. Cypermethrin, bisphenol A, galaxolide, tonalide, and versalide were found as the major stressors across key events of the studied pathway. Moreover, good correlations among key events validated the feasibility of method to predict *in vivo* response, suggesting that considering bioavailability and AOP improved environmental relevance for toxicant identification in a complex mixture.

* Corresponding author.
E-mail address: youjing@jnu.edu.cn (J. You).

https://doi.org/10.1016/j.jhazmat.2019.121853
Received 28 August 2019; Received in revised form 30 October 2019; Accepted 8 December 2019
Available online 16 December 2019

1. Introduction

Over 143 million chemicals have been indexed in American Chemical Society's Chemical Abstract (American Chemical Society, 2019), with approximately one million of those being commercially available (Daughton, 2005). Thus, it is no surprise that chemical mixtures are prevalent in various environmental media globally, and aquatic systems are no exception (Kortenkamp and Faust, 2018). Although a multitude of chemicals are present in aquatic systems, only a few are regularly monitored for regulatory purposes (*i.e.* the "priority/targeted list"). In general, these targeted lists are quite small, for example, China listed 68 chemicals as "priority contaminants" for monitoring in aquatic environment (Zhou et al., 1991). As such, assessing causality solely based on targeted analysis in many cases is either ineffective or biased towards the targeted chemicals (Escher et al., 2014; Cheng et al., 2017). To address the challenges associated with the complex mixtures, effect-directed analysis (EDA) has been developed to identify toxicants with known and unknown identities by integrating sample fractionation, bioassay, and chemical analysis (Brack, 2003).

Bioassays, either *in vivo* or *in vitro*, are critical for linking chemical exposure to ecological outcomes as part of the current EDA practices (Brack et al., 2016), but unfortunately both types of bioassays have their limitations. Although *in vivo* bioassays provide more regulatory concerned evaluations of toxicity at individual or population level (Di Paolo et al., 2015; Li et al., 2018; Hu et al., 2015; Raptis et al., 2014), their utilization has been hindered by low throughput, low sensitivity, and large sample volume requirements (Brack et al., 2016). Alternatively, high throughput *in vitro* bioassays have been widely applied in EDA, yet extrapolation of results from these assays to environmentally relevant outcomes is still challenging (Brack et al., 2016; Hong et al., 2016). To promote the EDA applications for regulatory purposes, it is imperative to bridge the gap between measured endpoints to realistic outcomes through developing toxicity pathway-guided multi-level bioassays and *in vitro* to *in vivo* extrapolations (IVIVE).

Additionally, identifying chemicals of concern in a mixture is highly dependent on endpoint choice, as improper selection can result in a biased determination of key toxicants. Non-specific cellular responses are more relevant to *in vivo* effects compared with subcellular specific/responsive endpoints, while the latter are directly related to molecular initiating events. To more thoroughly evaluate the risk of chemicals with various modes of action (MoAs), Escher and Hermens (2002) recommended to use a battery of endpoints in bioanalytical monitoring. Although adverse effects associated with non-specific (*e.g.*, cell viability (Qu et al., 2011)), specific (*e.g.*, estrogenic activity (Creusot et al., 2013; Liscio et al., 2014)), and responsive MoAs (*e.g.*, oxidative stress (Li et al., 2013a)) were individually used as toxicity endpoints in EDA, they have never been collectively utilized for diagnosing causality under the guidance of adverse outcome pathways (AOPs). To date, most EDAs have solely used xenobiotics metabolism pathway or hormone response as *in vitro* endpoints (Brack et al., 2016; Escher et al., 2015). As a consequence, a majority of identified toxicants in these studies have been those eliciting highly specific MoAs, such as aryl hydrocarbon receptor active, estrogenic, and androgenic compounds (Yue et al., 2015; Xiao et al., 2016; Hong et al., 2015; Weiss et al., 2009; Muschket et al., 2018). Though it may be sufficient in some circumstances, conducting bioassays with an arbitrarily pre-determined single endpoint could result in either no identification or an inaccurate identification of causality in complex ecosystems, where multiple stressors are present (Tang et al., 2013). Instead, it is beneficial to characterize toxicant category through AOP-directed screening before selecting specific and/or responsive endpoints for EDA in various scenarios. This could be accomplished by utilizing a battery of endpoints representing various AOP key events. Cellular responses of various cell lines might shed light on main AOPs of test mixtures and provide critical information for selecting appropriate endpoint battery in bioassays, as individual cell lines have inherent susceptibility to various compounds.

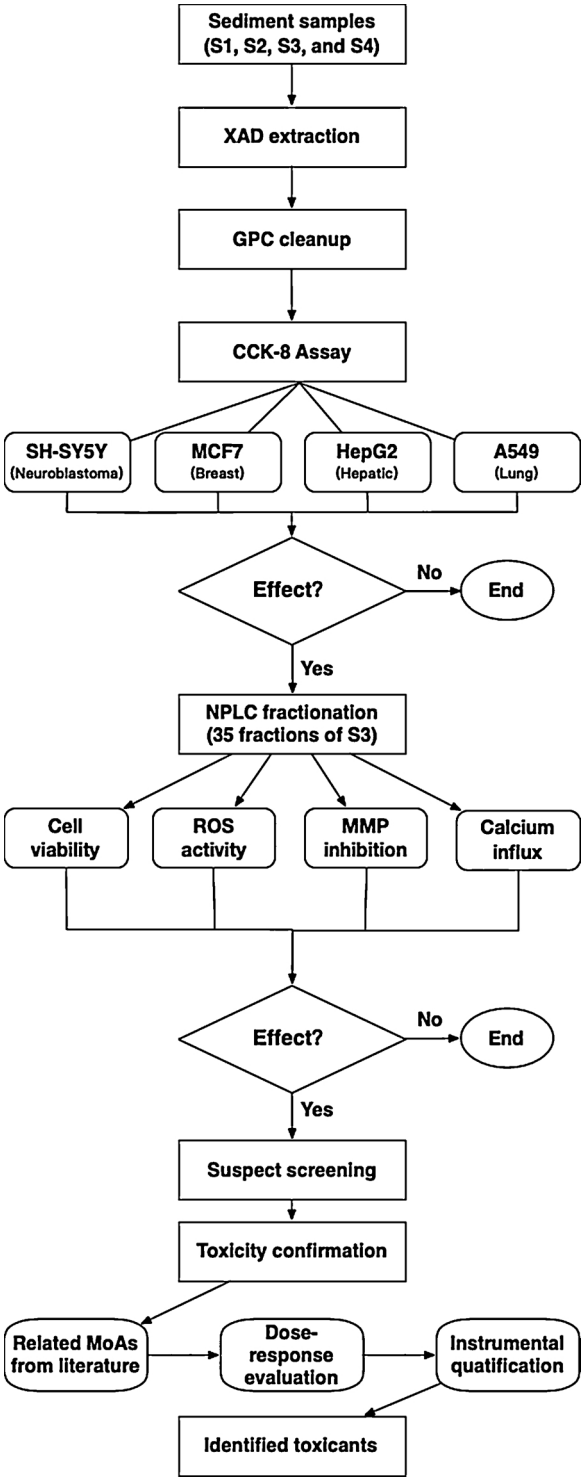

Fig. 1. Flowchart of the adverse outcome pathway (AOP) directed analysis approach. The procedures included bioaccessibility-based XAD extraction, cell sensitivity screening assays (CCK-8 tests with various cell lines), normal phase liquid chromatography fractionation, neurotoxicity AOP-guided assays using multiple endpoints (cell viability, reactive oxygen species (ROS) activity, mitochondrial membrane potential (MMP) inhibition, and calcium influx), suspect screening in the active fractions, and toxicity confirmation *via* chemical quantification and dose-response relations.

The aim of the current study was to develop an AOP-guided EDA method that utilized multiple *in vitro* endpoints as a means to unravel the principal toxicants in urban sediments which were potentially impacted by multiple stressors. In doing so, identified toxicants would not

be limited to certain groups of contaminants as a result of arbitrary pre-selection of endpoints. Four human cell lines (lung, liver, breast, and bone marrow) were used in the screening bioassays to categorize main AOP of the toxicants present in the sediment samples. These results were then served as the basis for selecting a battery of toxicity endpoints in subsequent AOP-guided EDA. Meanwhile, XAD resins were used to extract bioaccessible organic contaminants in sediment samples. To validate this method, sediments from urban waterways in Guangzhou, China, which were previously evaluated using *in vivo* endpoints (Qi et al., 2017), were assessed using this approach.

2. Materials and methods

2.1. Experimental design

Fig. 1 shows stepwise procedures of the newly developed EDA method, which utilized a bioassay with multiple *in vitro* endpoints and considered both bioaccessibility and AOP of toxicants. Four sediment samples were collected from urban waterways in Guangzhou, China. Bioaccessible fractions of contaminants in the sediments were extracted using XAD resins (Supelco) and these extracts were purified with gel permeation chromatography (GPC). Cell viability of four cell lines, including neuroblastoma (SH-SY5Y), breast cancer (MCF7), hepatic cancer cell (HepG2), and lung cancer cells (A549) to the XAD extracts was evaluated using cell count kit-8 (CCK-8) assays. The cell line showing significant cellular responses (SH-SY5Y) was subsequently examined using AOP-guided EDA procedure for the effects of individual fractions that were fractionized *via* normal phase liquid chromatography (NPLC). Cell viability and several AOP key event endpoints were tested. Suspect toxicants were identified in the fractions eliciting adverse effects and toxicity contributions of these suspects were evaluated by constructing dose-response relationships with neat compounds. Further information for individual steps is detailed below and in the Supplemental Information.

2.2. Sediment collection, extraction, and fractionation

Urban waterways in Guangzhou (the largest city in South China) were severely deteriorated by a variety of contaminants (Li et al., 2011; Mehler et al., 2011). Recently, a sediment toxicity identification evaluation (TIE) study in this area showed that organic pollutants were the main drivers for sediment toxicity to benthic invertebrates (Yi et al., 2015), however, in that study as well as subsequent studies only a portion of the observed effects could be explained by targeted analysis (Cheng et al., 2017). Therefore, further screening processes were employed to determine the contribution from toxicants that are not regularly monitored. For example, *in vivo* testing based EDA studies for this area indicated that current-use insecticides and synthetic musks were the major risk stressors to benthic invertebrates (Qi et al., 2017; Li et al., 2019).

The locations of the four sediment samples collected from urban waterways in Guangzhou, and information pertaining to the location of control sediment can be found in Table S1. To incorporate bioaccessibility of organic contaminants in sediment into EDA testing, bioaccessibility-based extraction with XAD resin was applied following a previously developed method (Li et al., 2019). As illustrated in previous studies (You et al., 2011; Li et al., 2013b; You and Li, 2017), bioaccessible fractions of organic contaminants better explained sediment toxicity than the total sediment concentrations, and XAD resin-assisted desorption has been shown an effective way to gain bioaccessible fractions of contaminants from sediment (Carroll et al., 1994; Lei et al., 2004). The bioaccessible fraction of sediment-associated contaminants was extracted using a mixture of XAD-2 and XAD-4 resins. In brief, 500 g of wet sediment, 500 mL of reconstituted water, and 20 g of XAD resins were added into a 1000-mL flask and stirred at 800 rpm for 24 h in darkness. At the end of 24-h extraction, XAD resins were separated from the sediment slurry and washed with deionized water three times. The contaminants in the resins were extracted by sonication with 50 mL of acetone once and an additional three cycles of 50 mL of hexane and acetone (1:1, v/v). All extracts were combined, filtered, and solvent exchanged to 4 mL of dichloromethane. These fractions were then purified using a semi-preparative GPC column packed with BioBeads S-X3, and this GPC-cleaned XAD extract was used in cell viability testing and EDA fractionation. Further details regarding the procedures for sediment collection, extraction, and fractionation are provided in (Li et al. (2019)) and in the Supplementary Information.

2.3. In vitro bioassays

2.3.1. Cell viability

Key events of respective endpoints as the evidence and cell viability as the downstream of adverse outcome were simultaneously tested. Four commercially available human cell lines, including SH-SY5Y, MCF7, HepG2, and A549 were cultured in the laboratory and used for bioassays. Cell types, testing endpoints, and detailed assay conditions are presented in **Table S2**. Using CCK-8 assays (Dojindo, Japan), cell viability of the four cell lines were evaluated after being exposed to XAD extracts from the collected sediments, Additionally, negative (XAD extracts of the control sediment) and blank controls (empty wells) were also included in the CCK-8 assays for quality control. Cell viability were calculated from the absorbance of the test sample (A_s), the negative control (A_c), and the blank control (A_b) using Eq. (1). Further details regarding the methods of cell culturing and CCK-8 bioassays are presented in the Supplemental Information.

$$\text{Cell viability} = \frac{A_s - A_b}{A_c - A_b} \times 100\% \quad (1)$$

Adverse effects on cells from the various functioning tissues provides insight into the initial events of stressors present in these extracts, which led to a more accurate specific/responsive endpoint selection in the bioassay screening. Significant cellular response was noted for SH-SY5Y cell line in the screening bioassay, as such calcium influx, mitochondrial membrane potential (MMP) inhibition, and reactive oxygen species (ROS) activity were assessed as neurotoxic key event of endpoints in subsequent screening. This information for each of the fractions was paired with additional CCK-8 tests to measure effects of downstream adverse outcome for each fraction.

2.3.2. Reactive oxygen species (ROS) activity

Elevated ROS activity indicated oxidative stress in SH-SY5Y cells, activity in this assays was quantified using a 2,7-dichlorodihydrofluorescein diacetate (DCFH-DA) fluorescent probe (Bass et al., 1983). Xanthine, the extract of control sediment, and empty wells in the plates were used as positive, negative, and blank controls, respectively, for assessing ROS activity (Miyachi et al., 1986). The ROS activity was calculated from the fluorescence value of test sample (F_s), negative control (F_c), and blank control (F_b) using Eq. (2) below. Additional information for measuring ROS activity in SH-SY5Y cells can be found in the Supplemental Information.

$$\text{ROS activity} = \frac{F_s - F_b}{F_c - F_b} \times 100\% \quad (2)$$

During toxicity confirmation steps, a flow-cytometer (BD FACSCalibur, New York, USA) was utilized to quantify ROS activity of suspect toxicants. Accumulation of redox compounds in the cells was quantified as an increase of fluorescence at 530 nm with exciting wavelength set at 485 nm (Eruslanov and Kusmartsev, 2010).

2.3.3. Mitochondrial membrane potential (MMP)inhibition

Dysfunction of mitochondrial was measured by the change of mitochondrial membrane potential using JC-1 fluorescent probe (Smiley et al., 1991). A dual-fluorescence intensity test was performed with one

excitation and emission wavelength pair at 485 and 530 nm, respectively, and another pair of excitation and emission wavelength at 485 and 590 nm, respectively. Then, the ratios of fluorescence intensity of J-aggregates ($F_{485,590}$) to monomer ($F_{485,530}$) for test sample (R_s), negative control (R_c), and blank control (R_b) were used to quantify mitochondrial membrane potential change following Eq. (3).

$$\text{MMP inhibition} = (1 - \frac{R_s - R_b}{R_c - R_b}) \times 100\% \quad (3)$$

2.3.4. Calcium influx

Calcium influx was loaded by Fura-2 AM fluorescent probe (Roe et al., 1990) and measured fluorescence ratio with the excitation wavelength at 340 and 380 nm and emission wavelength at 510 nm. The concentration of intracellular calcium ($[Ca^{2+}]$) was calculated following Eq. (4), and calcium influx was calculated as the ratio of $[Ca^{2+}]$ for the test and negative control samples ($[Ca^{2+}]_s$ and $[Ca^{2+}]_c$, respectively) using Eq. (5).

$$[Ca^{2+}] = K_d \times \frac{F_{340}}{F_{380}} \times \frac{R - R_{min}}{R_{max} - R} \quad (4)$$

$$\text{Calcium influx} = \frac{[Ca^{2+}]_s}{[Ca^{2+}]_c} \times 100\% \quad (5)$$

Where, K_d is dissociation constant with 224 nmol/L, and F_{340} and F_{380} represent fluorescence intensity of ion-bound and ion-free indicators, respectively, and they are measured at 340 and 380 nm, respectively. In addition, R is fluorescence intensity ratio and R_{max} and R_{min} stand for the maximum and minimum, respectively, of the ratios. More detailed information about the calcium influx measurements can be found in the Supplemental Information.

2.3.5. Bioassay parameters

For quality control, three blank controls (empty wells), three negative controls, and three positive controls were included in each 96-well plate for all bioassays. The 10 % and 50 % effect concentration (EC10 or EC50, respectively) was estimated by log-logistic dose response relationship.

Cypermethrin was used as the reference chemical for the CCK-8 assays. When estimating the effect concentration (ECx) of test samples, relative enrichment factors (REF) were used as dose metrics to construct the dose-response relationships (Neale et al. (2015)). The REF was calculated by multiplying a enrichment factor during sediment extraction by a dilution factor during *in vitro* bioassays (Eq. (6)). More details on REF calculation are shown in the Supplemental Information.

$$\text{REF} = \text{Enrichment factor} \times \text{Dilution factor} \quad (6)$$

2.4. Toxicant identification and confirmation

Potential toxicants in the active fractions, which showed significantly different effects from control, were screened using a Shimadzu GC–MS semi-quantification method for 942 pollutants using compound composer software (Shimadzu QP-2010 plus, Kyoto, Japan) (Qi et al., 2017). More details on the analytical methods are provided in the Supplemental Information.

A tiered confirmation approach was then conducted which involved MoA determination (*via* a literature search), bioactivity confirmation by constructing dose-response relationship to determine the toxicity of suspect toxicants in the active fractions using bioassays from neat compounds, followed by risk confirmation. In risk confirmation, the concentrations of candidate toxicants were quantified in field samples and compared to dose-response relationship constructed using neat compounds, and eventually toxicity contribution of suspect chemicals was predicted. This technique was utilized to further narrow the list of suspect toxicants (Fig. 1). To do so, information pertaining to the MoA of individual candidate toxicants in the active fractions was surveyed. Those that had the potential to affect the neurotoxicity pathways was regarded as suspect toxicants and further evaluated in the following tier. Those toxicants that fit the neurotoxicity AOP were evaluated using dose-response relationships to determine the associated EC10 or EC50 for the suspected toxicants in the fractions. These assays were conducted for cell viability and the key AOP events to confirm their potency. These ECx values were then used to determine the toxicity contribution of each suspect toxicant in the field samples, along with chemical quantification of candidate chemicals in the field samples. More information on the confirmation procedures using the dose-response curves, chemical quantification, and toxicity contribution are detailed below.

Neat compounds of the candidate toxicants were dissolved in dimethyl sulfoxide (DMSO) and the solutions were used for constructing dose-response relationships for individual suspects in cell viability, ROS, MMP, and calcium influx assays (operational procedures for the assays were discussed above). In addition, sediment samples were extracted using accelerated solvent extraction with a mixture of hexane and acetone (1:1, v/v) and the extracts were cleaned using solid phase extraction. The concentrations of suspect toxicants in the extracts were determined using a Shimadzu TQ-8040 GC–MS/MS (Shimadzu Corporation, Kyoto, Japan) and Triple Quad 5500 LC–MS/MS (AB SCIEX, USA). Detailed methods for sediment sample preparation and instrumental analysis are presented in the Supplemental Information.

Bioanalytical equivalent quantities were determined based on bioassays (BEQ_{bio}) and chemical analysis (BEQ_{chem}) and were used to evaluate toxicity contribution of individual toxicants (Escher et al., 2015). As shown in Eq. (7), BEQ_{bio} was calculated as the ratio of the ECx values of the reference chemical to the cleaned extracts (EC_{50} was used in initial screen testing and EC_{10} was used during toxicity confirmation).

$$BEQ_{bio} = \frac{ECx_{\text{ref chemical}}}{ECx_{\text{cal by REF}}} \quad (7)$$

Concurrently, $BEQ_{chem,j}$ values were calculated for individual suspect toxicants by multiplying measured concentrations of the chemical (*j*) in the test sample (C_j) to the ratio of the ECx values for the reference chemical ($ECx_{ref\ chemical}$) and the suspect toxicant (Ecx_j) using the same bioassay endpoints (Eq. (8)). Cypermethrin was selected as the reference chemical for the cell viability, ROS activity, MMP inhibition, and calcium influx assays.

$$BEQ_{chem,j} = C_j \times \frac{ECx_{\text{ref chemical}}}{ECx_j} \quad (8)$$

At last, toxicity contribution of each suspect toxicant (*j*) to the observed toxicity was calculated following Eq. (9)

$$\text{Toxicity contribution}_j = \frac{BEQ_{chemj}}{BEQ_{bio}} \quad (9)$$

2.5. Statistical analysis

Data analysis was performed using R software (version 3.41). Statistical difference between the treatments and the controls was evaluated using a one-way analysis of variance (ANOVA) followed by post-hoc Tukey Honest Significant Difference multiple comparison test (Tukey HSD). A two-way ANOVA was performed to assess differences in sensitivity amongst cell types in the initial cellular response screening assays. Dose-response relationships and associated ECx values were determined using a log-logistic model *via* the *drc* package (Ritz et al., 2016). Correlations between contaminant concentrations and toxic responses were determined using linear regression analysis. Principal component analysis (PCA) was performed to estimate the major contributors in the suspect toxicant list. Multi-correlation was conducted to

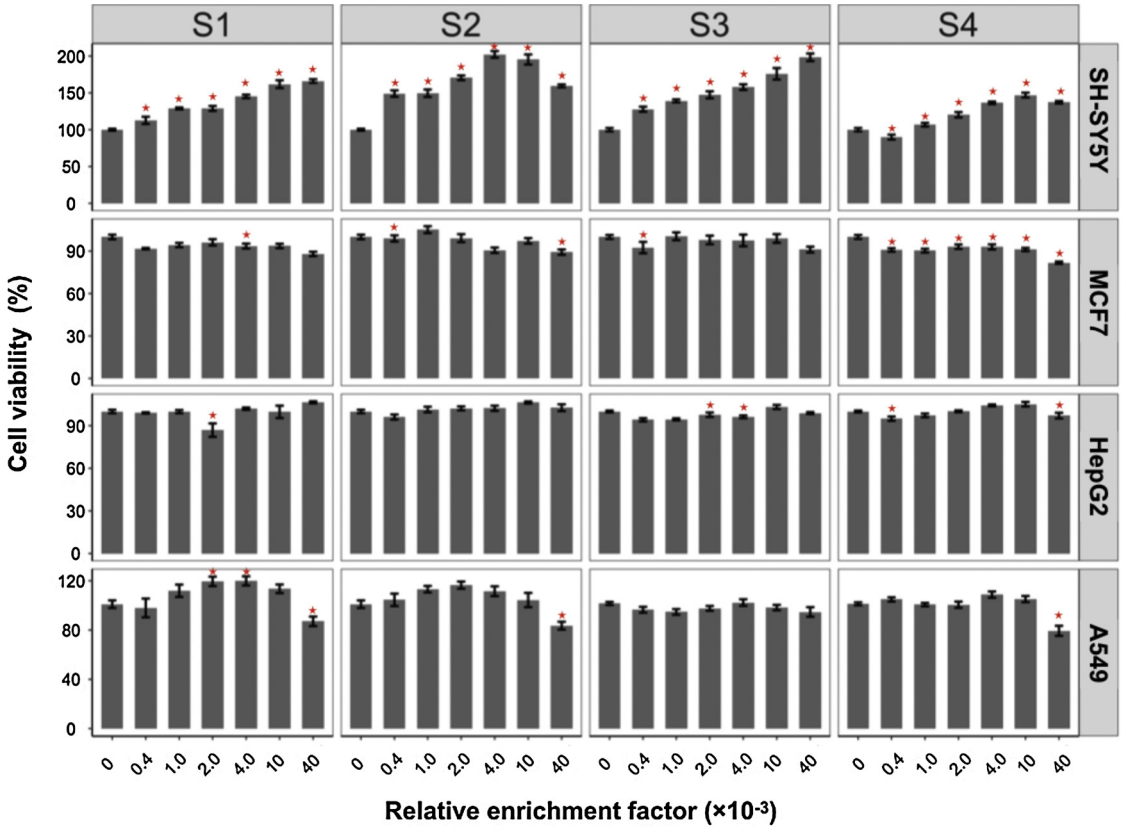

Fig. 2. Cell viability of SH-SY5Y, MCF7, HepG2, and A549 cell lines after exposure to XAD extracts of sediments collected from urban waterways in Guangzhou, China (S1–S4). Assays were conducted using XAD extracts with relative enrichment factors (REFs) of 4.0×10^{-4}, 1.0×10^{-3}, 2.0×10^{-3}, 4.0×10^{-3}, 1.0×10^{-2}, and 4.0×10^{-2}. Significant difference between the treatment and the control is indicated by a star (★).

validate the correlation between the responses of bioassays.

3. Results and discussion

3.1. Cell sensitivity guided screening testing

As shown in Fig. 1, cell viability of the GPC-purified XAD extracts of S1–S4 sediments were assessed using four cell lines: SH-SY5Y, MCF7, HepG2, and A549. Cell viability of the extracts were analyzed *via* CCK-8 assays at six REF_{XAD} values of 4.0×10^{-4}, 1.0×10^{-3}, 2.0×10^{-3}, 4.0×10^{-3}, 1.0×10^{-2}, and 4.0×10^{-2} (Fig. 2 and Table S3). All extracts at all REFs triggered significant growth of human neuroblastoma (SH-SY5Y) compared with negative control ($p < 0.05$) except of S4 at a REF of 4.0×10^{-4}, which slightly inhibited cell growth. In general, cell proliferation intensified with increasing doses, yet the responses started to decrease at the highest REF for sediments S2 and S4 (Fig. 2). In fact, nearly 200 % cell proliferation occurred for S2 (202 % and 195 % at REF of 4.0×10^{-3} and 1.0×10^{-2}, respectively) and S3 (198 % at REF of 4.0×10^{-2}). Comparatively, cell proliferation was less pronounced in sediments S1 and S4, with maximum cell proliferation of 166% and 137%, respectively (Table S3). The EC50 s for the extracts S1 − S4 were determined based on REF and were 2.31×10^{-3}, 4.06×10^{-4}, 1.81×10^{-3}, 2.00×10^{-1}, respectively. These EC50 values were used as references in preparing effective doses for subsequent bioassays. Additionally, BEQ_{bio} (SH-SY5Y cell viability) of samples S3 were calculated for toxicity confirmation and were 5.59×10^{5} μg/L.

In addition to affecting SH-SY5Y, the extract of sediment S4 remarkably inhibited the growth of MCF7 cells, showing a significant dose response relationship (Fig. 2). Conversely, the extracts of sediments S1–S3 showed little effect to the viability of MCF7 cells, with only several treatments being sporadically different from the controls. Human hepatic cancer cells HepG2 and lung cancer cells A549 were not affected by any sediment evaluated (Fig. 2).

To understand detrimental effects of chemical mixtures in water quality monitoring, researchers assembled a battery of assays according to AOPs to establish the causal relationship using key events as multiple lines of evidence (Escher and Hermens, 2002; Neale et al., 2017). In addition, AOP guidelines suggested that it should not neglect sensitivity difference of various cell lines (OECD, 2016). Therefore, an AOP-guided bioassay battery along with cell sensitivity screening testing was integrated into the current EDA, which provided more holistic understanding of sediment toxicity. To categorize the outcomes associated with different AOPs, systemic toxicity (neurotoxicity, endocrine disruption, and respiratory toxicity) and synthetic toxicity (hepatic toxicity) were evaluated in the initial screening cellular assays using SH-SY5Y, MCF7, A549, and HepG2 cell lines. A two-way ANOVA was performed using cell type as the nominal covariable, and significant differences in the observed effects among the four cell lines ($p < 0.01$) implied sufficiency of considering cell sensitivity. Overall, all of the four sediment extracts caused abnormal proliferation of the SH-SY5Y cell line, and one sediment (S4) also inhibited the growth of MCF7 cells. The results from the screening assay suggested that neurotoxicity was the sensitive pathway and should be further addressed.

3.2. AOP-directed analysis

3.2.1. Neurotoxicity-related endpoint selection

The goal of combining AOP information using multiple endpoints and utilizing this information for proper endpoint selection can greatly improve the accuracy of toxicant identification, as well as the applicability of EDA in various scenarios. Increased cell division may be provoked through non-specific pathways, like cell membrane

dysfunction, as a result of chemical accumulation in the phospholipids of the cells (Cerottini and Brunner, 1974). Moreover, cell cycle disorder which is related to specific or responsive pathways may also trigger increased cell division (Radi et al., 1991; Lowe et al., 1993). Therefore, the use of AOP-based multiple-endpoint bioassays, including cell viability and additional specific/responsive endpoints, as part of EDA practices can provide more solid evidence for diagnosing causality compared with a single endpoint of cell viability.

Cellular response of SH-SY5Y cells was detected in the cell sensitivity screening assays for all sediment samples. In addition, previous studies in the same area (Qi et al., 2017; Li et al., 2019) found neurotoxicants in sediment caused oxidative stress and contributed significantly to the observed midge mortality. Hence, a neurotoxicity-related AOP which contained ROS production and cellular response (AOP26 (AOPwiki, 2019)) was integrated into the current EDA to pinpoint sediment-bound neurotoxicants using human neuroblastoma SH-SY5Y. The AOP26 ("calcium-mediated neuronal ROS production and energy imbalance" (AOPwiki, 2019)) is depicted in Fig. S1. In brief, neurotoxicants could cause Ca^{2+} ATPase activity inhibition, intracellular calcium releases, mitochondrial dysfunction (MMP inhibition), and ROS generation in the neuroblastoma modulate cellular life cycle, which triggers impaired neurotransmission or oxidative neuronal damage (Barnham et al., 2004). This process is considered as a common pathway to induce outgrowth in neuroblastoma or apoptosis (Gawlik-Kotelnicka et al., 2016). Previous studies showed that this pathway would cause human neurodegeneration disease such as the Parkinson's and Alzheimer's disease (Emerit et al., 2004) and jeopardize aquatic organisms (Saari et al., 2017). Therefore, four key events of AOP26, including cell viability (proliferation or apoptosis), ROS generation (oxidative stress), MMP inhibition (mitochondrial dysfunction induced energy imbalance), and calcium influx (intracellular calcium releases) were chosen as the endpoints in further bioassays for the EDA fractions.

3.2.2. AOP26-guided EDA assays

Single specific endpoint has been commonly used in traditional EDA. This approach might overestimate toxicity contribution from chemicals with the selected specific MoA, as information on downstream key events is lack. Conversely, AOP was developed to support extrapolation among key events, which were used as the EDA endpoints. The choice of multiple endpoint regarding one AOP would strengthen the relationship of parallel testing. So, AOP-guided endpoint battery would be a promising diagnosis tool for assessing causality of mixture toxicity.

All four sediments impacted SH-SY5Y cells and sample S3 was chosen as the representative sample for the AOP26-guided EDA tests. The XAD extract of sediment S3 and its 35 individual NPLC fractions (N1–N35) were evaluated for cell viability using CCK-8 tests, ROS activity using DCFH-DA fluorescent probes, MMP inhibition using JC-1 probes, and calcium influx using Fura-2 AM probe and SH-SY5Y cells were used (Fig. 3 and Table S4). Here, cell viability and ROS generation were non-specific endpoints, while MMP inhibition and calcium influx were reactive and specific endpoints, respectively. The whole XAD extract of sediment S3 affected all of the four endpoints and dose-response relationships are presented in Fig. S2. An assumption has been proposed that the sediment consisted of chemicals acting on the AOP26 molecular initial event and further characterization would verify it by EDA fractionation and bioassays, suspect screening, and step-by-step confirmation.

Testing concentrations for individual fractions were determined based on cell viability EC50 value for the original extract of S3, with a REF of 1.81×10^{-3} (Table S3). As shown in Fig. 3, six fractions (N4, N20, N21, N22, N24, and N25) showed significant cell proliferation compared with the control in the CCK-8 testing, while two fractions (N10 and N30) significantly inhibited cell growth (cytotoxicity). The finding that nearly 20 % of the fractions (6/35) showed cellular responses for neuroblastoma SH-SY5Y supported the results for the raw extract in cell sensitivity screening testing. It should be noted that the responses in individual fractions were reduced in comparison to the raw extract, as would be expected from the fractionation process. The highest cell proliferation in the fractions was 108 % (N4), and it was lower than the result of raw extract (147 ± 15 %, Tables S3 and S4). Significant cytotoxicity was noted for N10 and N30, yet it was masked in the mixture without fractionation.

In addition to cell viability, more endpoints indicating AOP26 key events were also assessed for the 35 fractions. As presented in Table S4, nine fractions (N4, N10, N17, N19, N20, N21, N24, N25, and N31) significantly stimulated ROS generation. The highest ROS activity was noted in fractions N20 (133 %) and N21 (129 %) (Table S4). Interestingly, the distribution of effective fractions for ROS generation was similar to the cell viability, which showed significant responses in the fractions containing chemicals with a wide range of hydrophobicity (from N4 to N31). Meanwhile, nine fractions (N4, N5, N7, N8, N10, N12, N13, N16, and N17) caused significant MMP inhibition and a post hoc test showed only hydrophobic compounds (in the fractions with log $K_{ow} > 5.4$ based on the previous neat compounds validation (Li et al., 2019)) significantly induced MMP inhibition. Calcium influx is a specific endpoint and only four fractions (N10, N17, N21, and N34) significantly increased intracellular calcium. Within them, N10 showed the highest response (135 % compared with negative controls).

In summary, bioassay results of N10 fully paired to the AOP26, which showed increased intracellular calcium (135 %), MMP inhibition (75 %), ROS production (121 %), and cytotoxicity (87 %). Meanwhile, the fractions (N4, N17, and N21) that provided partial evidence (affecting three endpoints) also selected for suspect screening and toxicity validation. In consistent with the whole extract, N4 and N21 induced cell proliferation and ROS generation, but showed limited effect on calcium influx and MMP inhibition, respectively. Although N17 posed little effect on cell viability, it induced ROS generation, MMP inhibition, and calcium influx. Therefore, the four fractions (N4, N10, N17, and N21) were screened for candidate neurotoxicants.

3.3. Suspect toxicant identification and confirmation

3.3.1. Suspect identification

Suspect toxicants were screened in the N4, N10, and N21 fractions using a previously established GC–MS suspect screening method (Qi et al., 2017; Li et al., 2019). As shown in Table S5, 28 chemicals with a matching degree over 90 % similarity were identified in these fractions, with 10, 6, and 12 chemicals in N4, N10, and N21, respectively. Pesticides (> 67 %) were the most commonly detected compounds in these fractions.

The 28 chemicals were further evaluated for potential neurotoxicity for confirmation purposes. To do this, the MoA of these 28 chemicals was examined *via* a literature search and then compared to the AOP26, with a focus on cell viability, ROS generation, MMP inhibition, and intracellular calcium increase. As shown in Table S5, nine of the 28 compounds had no reported effects related to neurotoxicity pathways, and 12 compounds showed partial effects (at either cellular or subcellular level only). On the contrary, the rest seven chemicals, namely bisphenol A (BPA), 4-hydroxybenzaldehyde, cypermethrin, permethrin, fipronil, fipronil sulfone, and pyridaben have been reported to induce neurotoxicity related effects at both cellular and subcellular levels (Huang et al., 2016). These chemicals are highlighted by asterisks in Table S5 and were further validated using toxicity confirmation steps. A previous *in vivo* EDA study was conducted using the same sediment samples with a benthic invertebrate, *Chironomus dilutus* as test species and three synthetic musks (tonalide, galaxolide, and versalide) has been identified in fraction N17 (Li et al., 2019). Therefore, N17 was not included for suspect screening in the present study, instead, the three synthetic musks were added to the suspect list to validate if they acted through AOP26 to induce neurotoxicity.

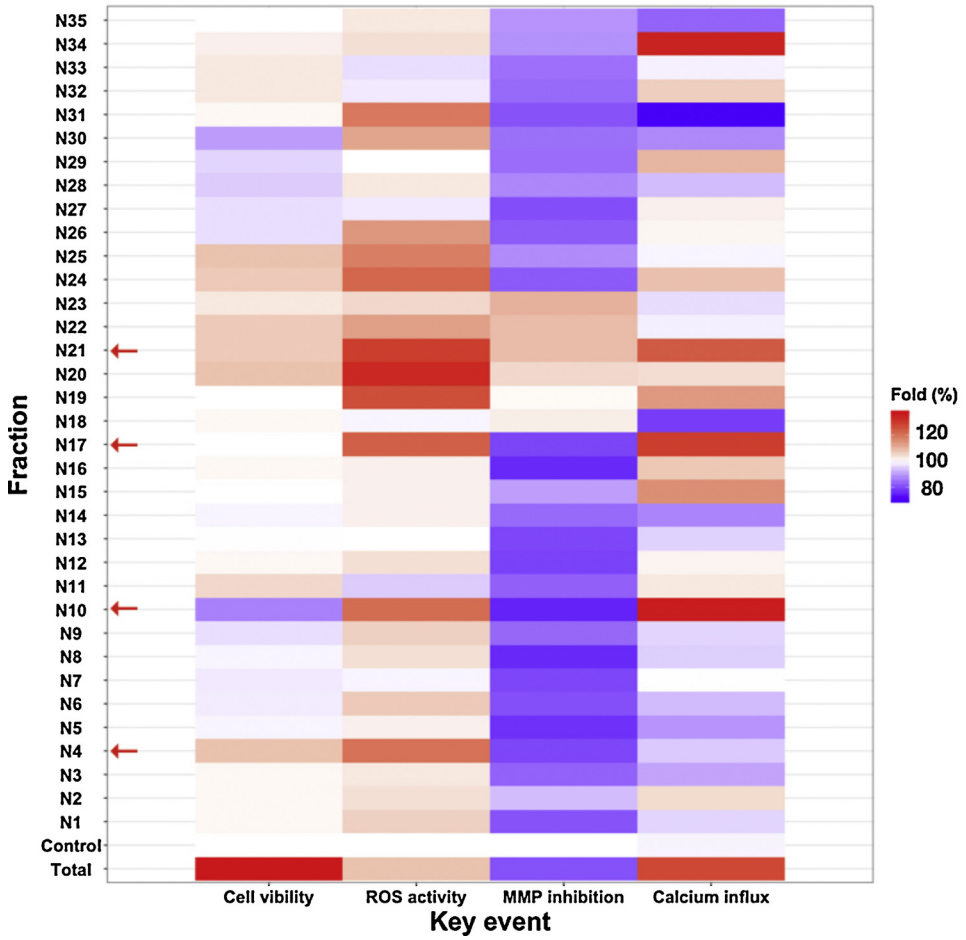

Fig. 3. Responses of the 35 fractionized extracts of sediment S3 for individual endpoints in the studied adverse outcome pathway. Neurotoxicity screening testing was conducted using human neuroblastoma SH-SY5Y, with cell viability, reactive oxygen species (ROS) activity, mitochondrial membrane potential (MMP), and calcium influx as toxicity endpoints.

3.3.2. Toxicity contribution estimation

To estimate toxicity contribution of individual suspects, the 10 suspect toxicants were further evaluated by the four toxicity endpoints in AOP-directed analysis and dose-response curves are presented in Fig. S3. The BEQ_{chem} values were calculated for individual suspects using toxic potency data and chemical concentrations in the four sediment extracts (Tables S6 and S7). The results were then compared with the effects observed for the sediment extract (BEQ_{bio}) to calculate toxicity contribution at each endpoint (Table S8).

All suspect toxicants in sediment showed limited effect on cell viability and the highest contribution was only 0.49 % by galaxolide in S4 (Table S8). As shown in Fig. S3, these compounds generally acted cytotoxicity instead of cell proliferation which was noted in sediment extracts, implying the presence of compounds which may induce cell proliferation and are not in the suspect screening list. Although the selected suspects posed little impact on cell viability, most chemicals induced remarkable ROS generation, which was a key event in AOP26. As shown in Table S8, the 10 suspects explained 10.2–14.0 % of ROS generation for the neuroblastoma in sediments S1–S4, and cypermethrin contributed to the most of ROS generation (64.2–95.5 % of the total), followed by galaxolide (11.5–29.3 %). As an upstream reactive effect, MMP inhibition was more selective than non-specific cell viability and ROS generation, and only six compounds showed measurable effects (Table S7). Within them, cypermethrin and galaxolide contributed to approximately 99 % of the total stress on energy imbalance caused by the suspects and explained 16.8 %–32.8 % of MMP inhibition noted in sediments S1–S4. Similarly, there were six compounds influencing the specific endpoint of calcium influx (Table S7). While the chemicals explained 12.0 %, 12.4 %, and 21.6 % of calcium influx response in sediments S1, S2, and S4, only about 1 % of calcium influx in S3 could be estimated by the chosen suspects. Different from other test endpoints, tonalide and BPA contribute the most to calcium influx and cypermethrin and galaxolide also played a role in this response.

To better illustrate toxicity contribution, PCA estimation was performed by supplementing the responses of all the sampling sites (Fig. 4). The 10 suspect toxicants were set as variance, with data from the four sites being grouped according to the four endpoints (cell viability, ROS activity, MMP inhibition, and calcium influx). All data were normalized using the ratio of BEQ_{chem} and BEQ_{bio} (Table S8). As shown in Fig. 4, data of cell viability and calcium influx showed focused distribution (with small size ellipses) while data of ROS generation and MMP inhibition were diverse (with big size ellipses). The difference might be induced by the wide detections of cellular and calcium influx responses and similar stressors responsive to them in the environment. Conversely, the situation of ROS generation and MMP inhibition indicated different responsive degree at each site and for different stressors. Two principal components with total 60.6 % explanation of the variances were selected. Among them, tonalide and BPA represented the highest loadings (cosine values of the vector with x axis) of PC1 with 0.13 and 0.12, respectively, coefficient of the 33.1 % score. In the meantime, galaxolide, cypermethrin, and versalide were with 0.24, 0.23. and 0.22 coefficient (cosine values of the vector with y axis), respectively, of PC2 (27.5 % score). As such, tonalide, BPA, galaxolide, cypermethrin, and versalide may explain 4.3 %, 4.0 %, 6.6 %, 6.3 %,

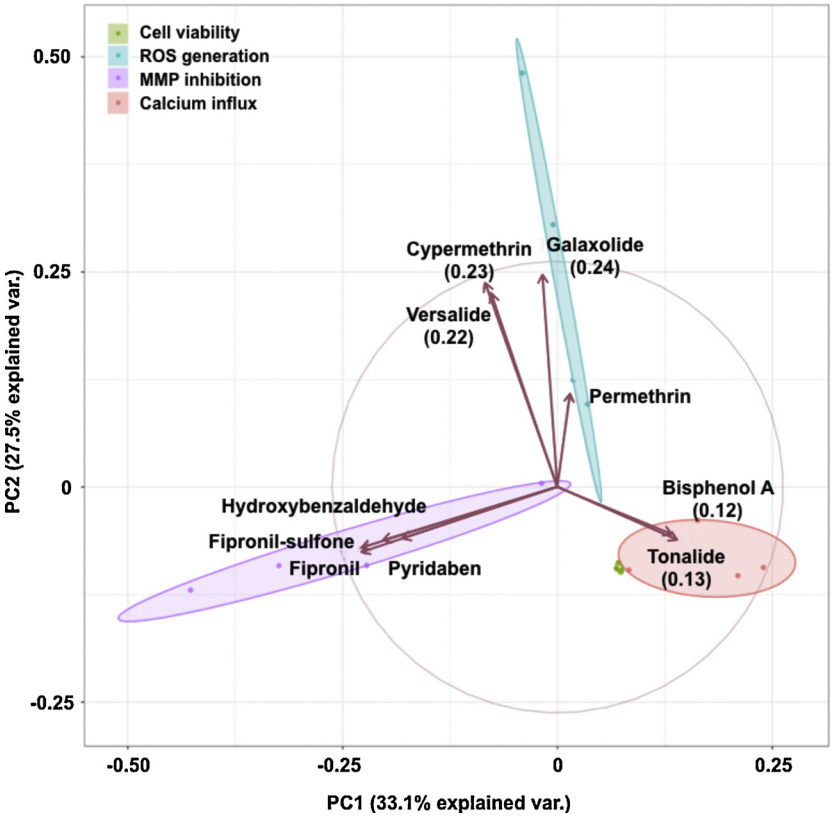

Fig. 4. Principle component analysis (PCA) biplot of ten suspect chemicals in the respective endpoints of neurotoxicity-screening to the observed effect. The four ellipses represented confidence intervals of the four point data (sampling sites in Guangzhou, China) for individual toxicity endpoints (cell viability, reactive oxygen species (ROS) generation, mitochondrial membrane potential (MMP) inhibition, and calcium influx) in the neurotoxicity related adverse outcome pathway. As the variances of analysis, the vector indicated a correlation to the two principle components by cosine values in the x and y axes.

and 6.1 % of the total endpoint-based variances at the sampling sites. While BPA was only showed evident response in calcium influx, cypemethrin and synthetic musks impacted all selected endpoints in AOP26 and were regarded as the major neurotoxicity contributors in sediment. Interestingly, the identified key toxicants in the current *in vitro* study were in accordance with those to midge mortality in a previous *in vivo* EDA study in the same area (Li et al., 2019).

3.4. In vitro to in vivo extrapolations (IVIVE)

To further validate the assumption that identified toxicants (tonalide, galaxolide, versalide, and cypermethrin) acted the intracellular calcium mediated neurotoxicity through AOP26 to induce the cell response and evaluate the applicability of IVIVE in aquatic risk assessment, a multi-correlation among *in vivo* and *in vitro* endpoints was analyzed (Fig. 5). All data (ratio of BEQ_{chem} to BEQ_{bio}) were logarithm-normalized to attain reasonable distribution for statistical analysis and the distribution was shown in the diagonal plots of Fig. 5.

As shown in Fig. 5, the step-by-step correlations between calcium influx and MMP inhibition ($r = 0.36$, $p < 0.05$), MMP inhibition and ROS generation ($r = 0.69$, $p < 0.05$), and ROS generation and cell viability ($r = 0.40$, $p < 0.05$) were all statistically significant, which validated the appropriateness of the endpoint battery in the neurotoxicity related AOP26 in sediment EDA analysis. Obviously, if the correlation between each endpoint was significant, a stressor would be existing by acting on both responses. So, the step-by-step correlation of the four responses indicated the occurrence of stressors contributed to all responses, and the assumption would be adequately validated that intercellular mediated neurotoxicity related AOP were induced by the key toxicants identified in the present study.

In the meantime, the strong correlation between *in vivo* midges mortality and *in vitro* MMP inhibition ($r = -0.49$, $p < 0.05$) and calcium influx ($r = -0.60$, $p < 0.05$) showed the feasibility of using IVIVE to gain organism-level outcome with low-cost high-throughput *in vitro* data. This was also confirmed by the result of the same toxicants being identified using both *in vitro* (the present study) and *in vivo* EDA (Li et al., 2019). It should be a remarkable guideline to increase environment relevance when using cell model testing.

Comparatively, correlation between the mortality of the midges and cell viability and ROS generation of human cells was poor. This indicated the necessity of developing aquatic organism cells for extrapolating toxic effect in aquatic species, and it should be a promising tool to combine high-through testing, AOP clarification, and environment relevance in aquatic EDA and risk assessment in the future.

4. Conclusions

Bioavailable extracts were prepared by XAD extraction from sediments of urban creeks in Guangzhou as a case study to validate a newly developed AOP-directed EDA approach. Neurotoxicity was determined to be endpoints of concern in cell sensitivity screening assays and were focused on subsequent bioassay evaluations. In the complex mixture, it was observed that stressors in these samples induced neurotoxicity. In subsequent AOP-guided EDA (for a sediment XAD extract), a total of 35 fractions were evaluated using a battery of causal endpoints (calcium influx, MMP inhibition, ROS activity, and cell viability). The *in vitro* EDA suggested that three synthetic musks and cypermethrin were the key contributors to neurotoxicity at subcellular and cellular levels. This study complimented and strengthened previous work that conducted EDA procedures using *in vivo* endpoints. Overall, this study shows the potential strength of using multiple endpoints within a AOP framework of uncovering key toxicants which were not regularly monitored, especially when these endpoints are taken in context of the AOP framework.

Declaration of Competing Interest

The authors declare no conflicts of interest.

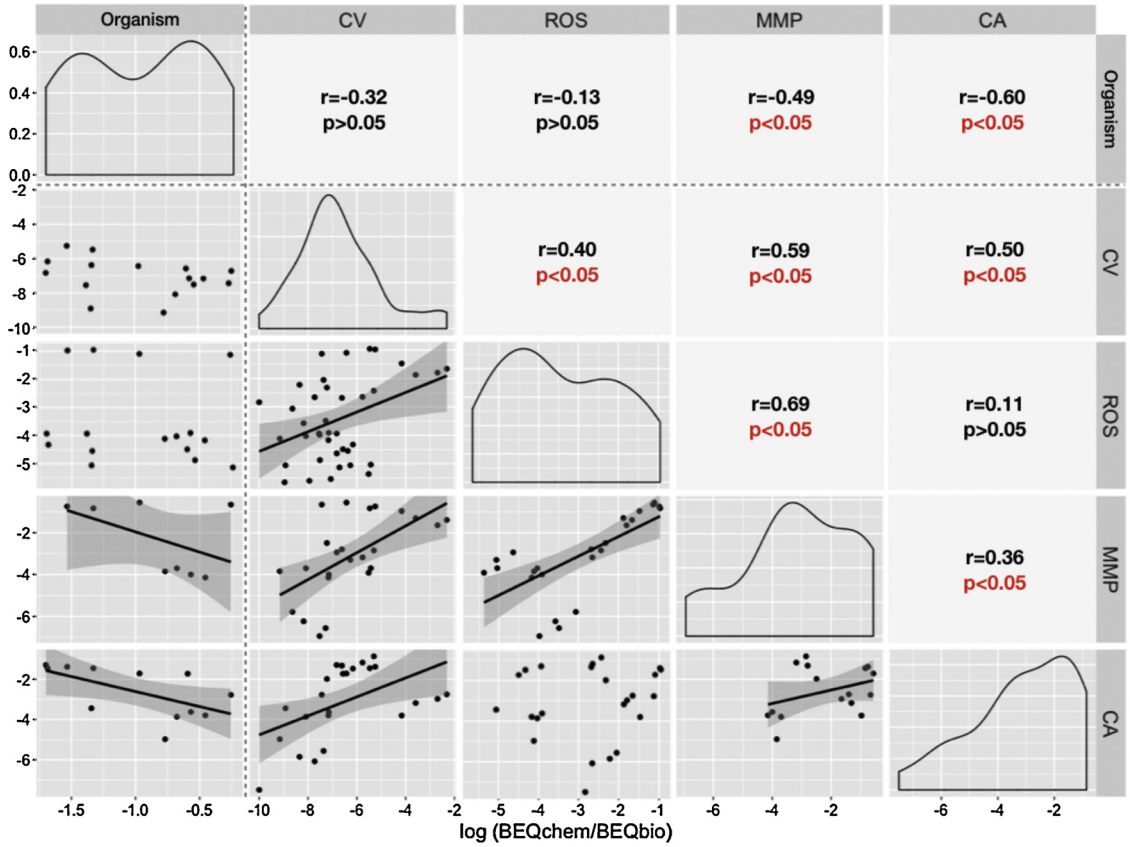

Fig. 5. Multivariate correlation relationships between the ratios of the observed bioanalytical equivalent quantity (BEQ_{bio}) to the predicted one (BEQ_{chem}) for pairs of endpoints in the neurotoxicity related adverse outcome pathway (organism-level midge mortality, cell viability, reactive oxygen species (ROS) generation, mitochondrial membrane potential (MMP) inhibition, and calcium influx). Diagonal plots showed data distribution of the logarithmic ratios. Lower plots showed scattering data, correlation (real line), and the respective confidence intervals (shadow). Upper plots presented the correlation coefficients (r) and p values, and significant correlations are indicated as $p < 0.05$.

Acknowledgements

This work was supported by the Ministry of Science and Technology of China (2017ZX07301005-002), the National Science Foundation of China (41977343 and 41773101), and Guangdong Provincial Department of Science and Technology (2017A020216002 and 2015TX01Z168). We would like to thank Dr. W.T. Mehler for his assistance with language edition. This is contribution No.IS-2787 from GIGCAS.

Appendix A. Supplementary data

Supplementary material related to this article can be found, in the online version, at doi:https://doi.org/10.1016/j.jhazmat.2019.121853.

References

American Chemical Society. (accessed on Jan 1, 2019). www.cas.org/index.
AOPwiki, 2019 https://aopwiki.org/aops/26 (accessed on Jan 1, 2019).
Barnham, K.J., Masters, C.L., Bush, A.I., 2004. Neurodegenerative diseases and oxidative stress. Nat. Rev. Drug Discov. 3, 205–214.
Bass, D.A., Parce, J.W., Dechatelet, L.R., Szejda, P., Seeds, M.C., Thomas, M., 1983. Flow cytometric studies of oxidative product formation by neutrophils: a graded response to membrane stimulation. J. Immunol. 130, 1910–1917.
Brack, W., 2003. Effect–directed analysis: a promising tool for the identification of organic toxicants in complex mixtures? Anal. Bioanal. Chem. 377, 397–407.
Brack, W., Ait-Aissa, S., Burgess, R.M., Busch, W., Creusot, N., Di Paolo, C., Escher, B.I., Mark Hewitt, L., Hilscherova, K., Hollender, J., Hollert, H., Jonker, W., Kool, J., Lamoree, M., Muschket, M., Neumann, S., Rostkowski, P., Ruttkies, C., Schollee, J., Schymanski, E.L., Schulze, T., Seiler, T.-B., Tindall, A.J., De Aragão Umbuzeiro, G., Vrana, B., Krauss, M., 2016. Effect–directed analysis supporting monitoring of aquatic environments – an in–depth overview. Sci. Total Environ. 544, 1073–1118.
Carroll, K.M., Harkness, M.R., Bracco, A.A., Balcarcel, R.R., 1994. Application of a permeant/polymer diffusional model to the desorption of polychlorinated biphenyls from Hudson River sediments. Environ. Sci. Technol. 28, 253–258.
Cerottini, J.-C., Brunner, K.T., 1974. Cell–mediated cytotoxicity, allograft rejection, and tumor immunity. In: Dixon, F.J., Kunkel, H.G. (Eds.), Advances in Immunology. Academic Press, pp. 67–132.
Cheng, F., Li, H., Qi, H., Han, Q., You, J., 2017. Contribution of pyrethroids in large urban rivers to sediment toxicity assessed with benthic invertebrates *Chironomus dilutus*: a case study in South China. Environ. Toxicol. Chem. 36, 3367–3375.
Creusot, N., Budzinski, H., Balaguer, P., Kinani, S., Porcher, J.-M., Ait-Aissa, S., 2013. Effect–directed analysis of endocrine–disrupting compounds in multi–contaminated sediment: identification of novel ligands of estrogen and pregnane X receptors. Anal. Bioanal. Chem. 405, 2553–2566.
Daughton, C.G., 2005. "Emerging" chemicals as pollutants in the environment: a 21st century perspective. Renew. Resour. J. 23, 6–14.
Di Paolo, C., Seiler, T.-B., Keiter, S., Hu, M., Muz, M., Brack, W., Hollert, H., 2015. The value of zebrafish as an integrative model in effect–directed analysis – a review. Environ. Sci. Eur. 27, 8–18.
Emerit, J., Edeas, M., Bricaire, F., 2004. Neurodegenerative diseases and oxidative stress. Biomed. Pharmacother. 58, 39–46.
Eruslanov, E., Kusmartsev, S., 2010. Identification of ROS using oxidized DCFDA and flow–cytometry. In: Armstrong, D. (Ed.), Advanced Protocols in Oxidative Stress II. Humana Press, Totowa, NJ, pp. 57–72.
Escher, B.I., Hermens, J.L.M., 2002. Modes of action in ecotoxicology: their role in body burdens, species sensitivity, QSARs, and mixture effects. Environ. Sci. Technol. 36, 4201–4217.
Escher, B.I., Allinson, M., Altenburger, R., Bain, P.A., Balaguer, P., Busch, W., et al., 2014. Benchmarking organic micropollutants in wastewater, recycled water and drinking water with in vitro bioassays. Environ. Sci. Technol. 48, 1940–1956.
Escher, B.I., Neale, P.A., Leusch, F.D.L., 2015. Effect–based trigger values for in vitro bioassays: reading across from existing water quality guideline values. Water Res. 81, 137–148.
Gawlik-Kotelnicka, O., Mielicki, W., Rabe-Jablonska, J., Lazarek, J., Strzelecki, D., 2016. Impact of lithium alone or in combination with haloperidol on oxidative stress parameters and cell viability in SH–SY5Y cell culture. Acta Neuropsychiatr. 28, 38–44.
Hong, S., Lee, S., Choi, K., Kim, G.B., Ha, S.Y., Kwon, B.-O., Ryu, J., Yim, U.H., Shim, W.J., Jung, J., Giesy, J.P., Khim, J.S., 2015. Effect–directed analysis and mixture effects of

AhR–active PAHs in crude oil and coastal sediments contaminated by the Hebei Spirit oil spill. Environ. Pollut. 199, 110–118.
Hong, S., Giesy, J.P., Lee, J.-S., Lee, J.-H., Khim, J.S., 2016. Effect–directed analysis: current status and future challenges. Ocean Sci. J. 51, 413–433.
Hu, X., Shi, W., Yu, N., Jiang, X., Wang, S., Giesy, J.P., Zhang, X., Wei, S., Yu, H., 2015. Bioassay-directed identification of organic toxicants in water and sediment of Tai Lake, China. Water Res. 73, 231–241.
Huang, F., Liu, Q., Xie, S., Xu, J., Huang, B., Wu, Y., Xia, D., 2016. Cypermethrin induces macrophages death through cell cycle arrest and oxidative stress–mediated JNK/ERK signaling regulated apoptosis. Int. J. Mol. Sci. 17, 885–897.
Kortenkamp, A., Faust, M., 2018. Regulate to reduce chemical mixture risk. Science 361, 224–226.
Lei, L., Suidan, M.T., Khodadoust, A.P., Tabak, H.H., 2004. Assessing the bioavailability of PAHs in field–contaminated sediment using XAD–2 assisted desorption. Environ. Sci. Technol. 38, 1786–1793.
Li, H., Tyler Mehler, W., Lydy, M.J., You, J., 2011. Occurrence and distribution of sediment–associated insecticides in urban waterways in the Pearl River Delta, china. Chemosphere 82, 1373–1379.
Li, J.-Y., Tang, J.Y.M., Jin, L., Escher, B.I., 2013a. Understanding bioavailability and toxicity of sediment–associated contaminants by combining passive sampling with in vitro bioassays in an urban river catchment. Environ. Toxicol. Chem. 32, 2888–2896.
Li, H., Sun, B., Chen, X., Lydy, M.J., You, J., 2013b. Addition of contaminant bioavailability and species susceptibility to a sediment toxicity assessment: application in an urban stream in China. Environ. Pollut. 178, 135–141.
Li, H., Zhang, J., You, J., 2018. Diagnosis of complex mixture toxicity in sediments: application of toxicity identification evaluation (TIE) and effect–directed analysis (EDA). Environ. Pollut. 237, 944–954.
Li, H., Yi, X., Cheng, F., Tong, Y., Mehler, W.T., You, J., 2019. Identifying organic toxicants in sediment using effect-directed analysis: a combination of bioaccessibility-based extraction and high-throughput midge toxicity testing. Environ. Sci. Technol. 53, 996–1003.
Liscio, C., Abdul-Sada, A., Al-Salhi, R., Ramsey, M.H., Hill, E.M., 2014. Methodology for profiling anti-androgen mixtures in river water using multiple passive samplers and bioassay-directed analyses. Water Res. 57, 258–269.
Lowe, S.W., Ruley, H.E., Jacks, T., Housman, D.E., 1993. p53–dependent apoptosis modulates the cytotoxicity of anticancer agents. Cell 74, 957–967.
Mehler, W.T., Li, H., Lydy, M.J., You, J., 2011. Identifying the causes of sediment–associated toxicity in urban waterways of the Pearl River Delta, china. Environ. Sci. Technol. 45, 1812–1819.
Miyachi, Y., Yoshioka, A., Imamura, S., Niwa, Y., 1986. Effect of antibiotics on the generation of reactive oxygen species. J. Invest. Dermatol. 86, 449–453.
Muschket, M., Di Paolo, C., Tindall, A.J., Touak, G., Phan, A., Krauss, M., Kirchner, K., Seiler, T.-B., Hollert, H., Brack, W., 2018. Identification of unknown antiandrogenic compounds in surface waters by effect–directed analysis (EDA) using a parallel fractionation approach. Environ. Sci. Technol. 52, 288–297.
Neale, P.A., Ait-Aissa, S., Brack, W., Creusot, N., Denison, M.S., Deutschmann, B., Hilscherová, K., Hollert, H., Krauss, M., Novák, J., Schulze, T., Seiler, T.-B., Serra, H., Shao, Y., Escher, B.I., 2015. Linking in vitro effects and detected organic micropollutants in surface water using mixture–toxicity modeling. Environ. Sci. Technol. 49, 14614–14624.
Neale, P.A., Altenburger, R., Aït-Aïssa, S., Brion, F., Busch, W., Umbuzeiro, G.D.A., Denison, M.S., Pasquier, D.D., Hollert, H., Morales, D.A., Novak, J., Schlichting, R., Seiler, T.-B., Serra, H., Shao, Y., Tindall, A.J., Tollefsen, K.E., Williams, T.D., Escher, B.I., 2017. Development of a bioanalytical test battery for water quality monitoring: fingerprinting identified micropollutants and their contribution to effects in surface water. Water Res. 123, 734–750.
OECD, 2016. Users' Handbook Supplement to the Guidance Document for Developing and Assessing Adverse Outcome Pathways. OECD publishing.
Qi, H., Li, H., Wei, Y., Mehler, W.T., Zeng, E.Y., You, J., 2017. Effect–directed analysis of toxicants in sediment with combined passive dosing and in vivo toxicity testing. Environ. Sci. Technol. 51, 6414–6421.
Qu, G., Shi, J., Wang, T., Fu, J., Li, Z., Wang, P., Ruan, T., Jiang, G., 2011. Identification of tetrabromobisphenol a diallyl ether as an emerging neurotoxicant in environmental samples by bioassay–directed fractionation and HPLC–APCI–MS/MS. Environ. Sci. Technol. 45, 5009–5016.
Radi, R., Beckman, J.S., Bush, K.M., Freeman, B.A., 1991. Peroxynitrite–induced membrane lipid peroxidation: the cytotoxic potential of superoxide and nitric oxide. Arch. Biochem. Biophys. 288, 481–487.
Raptis, C.E., Juraske, R., Hellweg, S., 2014. Investigating the relationship between toxicity and organic sum–parameters in kraft mill effluents. Water Res. 66, 180–189.
Ritz, C., Baty, F., Streibig, J.C., Gerhard, D., 2016. Dose–response analysis using r. PLoS One 1, 13–25.
Roe, M.W., Lemasters, J.J., Herman, B., 1990. Assessment of Fura-2 for measurements of cytosolic free calcium. Cell Calcium 11, 63–73.
Saari, G.N., Scott, W.C., Brooks, B.W., 2017. Global scanning assessment of calcium channel blockers in the environment: review and analysis of occurrence, ecotoxicology and hazards in aquatic systems. Chemosphere 189, 466–478.
Smiley, S.T., Reers, M., Mottola-Hartshorn, C., Lin, M., Chen, A., Smith, T.W., Steele, G.D., Chen, L.B., 1991. Intracellular heterogeneity in mitochondrial membrane potentials revealed by a J-aggregate-forming lipophilic cation JC-1. Proc. Natl. Acad. Sci. U. S. A. 88, 3671–3675.
Tang, J.Y.M., McCarty, S., Glenn, E., Neale, P.A., Warne, M.S.J., Escher, B.I., 2013. Mixture effects of organic micropollutants present in water: towards the development of effect–based water quality trigger values for baseline toxicity. Water Res. 47, 3300–3314.
Weiss, J., Hamers, T., Thomas, K., van der Linden, S., Leonards, P.G., Lamoree, M., 2009. Masking effect of anti–androgens on androgenic activity in European river sediment unveiled by effect–directed analysis. Anal. Bioanal. Chem. 394, 1385–1397.
Xiao, H., Krauss, M., Floehr, T., Yan, Y., Bahlmann, A., Eichbaum, K., Brinkmann, M., Zhang, X., Yuan, X., Brack, W., Hollert, H., 2016. Effect–directed analysis of aryl hydrocarbon receptor agonists in sediments from the Three Gorges Reservoir, China. Environ. Sci. Technol. 50, 11319–11328.
Yi, X., Li, H., Ma, P., You, J., 2015. Identifying the causes of sediment–associated toxicity in urban waterways in South China: incorporating bioavailabillity–based measurements into whole–sediment toxicity identification evaluation. Environ. Toxicol. Chem. 34, 1744–1750.
You, J., Li, H., 2017. Improving the accuracy of effect–directed analysis: the role of bioavailability. Environ. Sci.–Proc. Imp. 19, 1484–1498.
You, J., Harwood, A.D., Li, H., Lydy, M.J., 2011. Chemical techniques for assessing bioavailability of sediment–associated contaminants: SPME versus Tenax extraction. J. Environ. Monitor. 13, 792–800.
Yue, S., Ramsay, B.A., Brown, R.S., Wang, J., Ramsay, J.A., 2015. Identification of estrogenic compounds in oil sands process waters by effect directed analysis. Environ. Sci. Technol. 49, 570–577.
Zhou, W.F., Sun, Dqian, Zongguang, 1991. Determination of black list of China's priority pollutants in water. Res. Environ. Sci. 3, 18–20.